

Effects of MWCNTs Dispersion on the Microstructure of Sol-Gel Derived Hydroxyapatite

J. Jaafaripour Maybody¹, A. Nemati^{2*}, E. Salahi³, M. H. Amin³

1- Department of Materials Engineering, Islamic Azad University, Tehran, I. R. Iran

2- Department of Materials Science and Engineering, Sharif University of Technology, Tehran, I. R. Iran

3- Materials and Energy Research Center, Tehran, I. R. Iran

(*) Corresponding author: nemati@sharif.edu

(Received: 28 Feb. 2010 and Accepted: 02 Jun. 2010)

Abstract:

Stable homogeneous dispersions of carbon nanotubes (CNTs) were prepared using ethanol as dispersing agent. Then, using sol-gel method, dispersion in the hydroxyapatite matrix and its effects on the microstructure were investigated. The phase composition, chemical structure and morphological and size analyses were performed using XRD, FT-IR, SEM, TEM/SAED/EDX and Raman spectroscopy. The influences of different dispersing agents (sodium dodecyl sulfate (SDS) as a benchmark for future dispersion experiments) and excitation wavelength are discussed and the results are compared with the commonly used UV-Visible spectroscopic analysis. The results indicated that the synthesis of hydroxyapatite particles in the presence of carbon nanotubes had the best effect on the homogenization of carbon nanotube dispersion. The average crystallite size of heat-treated (at 600°C) samples, estimated by Scherrers equation, was found to be ~50-60 nm that was confirmed by TEM.

Keywords: Carbon Nanotube, Sol-Gel, FT-IR, SEM, TEM, UV-visible Spectroscopy

1. INTRODUCTION

Carbon nanotubes (CNTs) have been one attracted by several research groups in recent years. That is due to its remarkable structural, electrical, mechanical and thermal properties [1-3]. On aspect of these research efforts, however, has focused on developing their synthesis techniques and producing defect-free tubes for special applications that mainly take advantage of their electrical properties. Nowadays, the incorporation of nanotubes into ceramic and polymeric matrices is a vast area of study and research [3-7].

However, fabrication of homogeneous nanocomposites with carbon nanotubes remains

a technical challenge [9]. For example, a general problem associated with their application is their inherent insolubility in most solvents which is also a prerequisite for their application as additives for the reinforcement of composite materials. When reinforcement is incorporated into a matrix, the interface between the matrix and the reinforcement becomes extremely important. In fact, when CNTs reinforce a composite, the high stability becomes a shortcoming in the interaction between the matrix and the reinforcement.

Another noticeable difficulty that can hinder CNTs from becoming commercially applicable is their uncontrolled agglomeration due to their nanometer size (the large surface area). Therefore, effective dispersants and synthesis methods are needed

and sometimes are developed to produce carbon nanotube dispersions that are uniform in properties and stable over long periods of time [8-11]. Among many forms of calcium phosphate, hydroxyapatite ($\text{Ca}_{10}(\text{PO}_4)_6(\text{OH})_2$, HA) is one of the most well-known phases studied for a number of biomedical applications due to its outstanding biological responses to physiological environment and its very close similarity to natural bone structure [12-17]. The development of an HA/CNTs composite material is attractive as its advantageous properties of the combination of the osteoconductive property of HA and the excellent mechanical property of CNTs.

However, adding carbon nanotubes and hydroxyapatite composite directly to the traditional bone repair materials cannot meet the requirements of ideal bone tissue engineering scaffold materials. It is essential for bone tissue engineering scaffold materials that how to closely integrate with the surrounding bone tissue after implantation in the body. So, an HA layer of formation on the surface of CNTs to obtain nanohybrid will provide a composite material with superior performance for bone tissue engineering.

Since the bioactivity of CNTs was reported [18-20], their use in biomedical application has been anticipated. The most important issues in preparing CNTs/ceramic composites with high performances are homogenous mixing between CNTs and ceramic powders, retention of perfect structure of CNTs during preparation of composites, strong interfacial bonding between CNTs and matrix, and ensuring load translation. In the present study, carbon nanotubes was dispersed in the hydroxyapatite (HA) matrix using ethanol as dispersant and via sol-gel process and its effects on the microstructure were investigated.

2. EXPERIMENTAL

A multi-wall carbon nanotube (MWCNTs, diameter 10-30 nm, length 15-50 μm , Aldrich, product ID 636517) was used. The MWCNTs powder was cleaned in acetone and dehydrated at 200°C before

mixing with HA sol. In the sol-gel process, 0.5M phosphorus containing precursor was prepared by the addition of P_2O_5 (MERCK Art. No.540) to ethanol (MERCK Art. No.1.00971). The resulting ester was then refluxed at room temperature for 24 h. A solution of 1.67M $\text{Ca}(\text{NO}_3)_2 \cdot 4\text{H}_2\text{O}$ (MERCK Art. No. 2120) in ethanol was then prepared and mixed for 3h. The phosphorus containing precursor was added drop-wise to this solution, while it was being stirred vigorously. In a typical synthesis, the purified MWCNTs mentioned above were dispersed into ethanol (in a 10 mL solution of 1 wt% dispersant ethanol) by ultrasonic agitation in a bath sonicator (110W) for 30 min (at room temperature) to obtain a homogeneity.

It has been reported [18, 19] that ultrasonication is an external mechanical energy that helps the particles to overcome the attractive van der Waals force at contact. In the next step, MWCNTs sol, was added to HA sol and stirred vigorously (350 r.p.m) for 8 h at an ambient temperature. The sol was evaporated to increase the viscosity to obtain gels. In fact, the solvent was first evaporated to form a gel, then organic components in the gel were decomposed.

Finally, the mixture was burnt to become as-prepared powders. The obtained gels were dried at 120°C for 24 h in an electrical air oven. The dried gels were individually heated in the range of 5°C/min up to 600°C for 2 h in a muffle furnace in order to obtain HA-MWCNTs mixed powder. Crystallinity of the MWCNTs-HA samples was characterized by X-ray diffractometer equipped with CuK_α source and operating at 40 KV and 40 mA, obtained at a scan rate of 2 degrees per min. A Fourier transform infrared spectrum (FT-IR, Bruker, Vector 33) using KBr pellets in the range of 4000-400 cm^{-1} at room temperature was used.

The morphology of the selected resulting powders was examined with scanning electron microscope (SEM, XL30, Philips, Holland) operating at 25 KV. Finally, transmission electron microscopy (TEM, CM200FEG, Philips) and Raman spectroscopy were carried out to characterize the particles and CNTs. CNTs dispersions are commonly quantified or characterized by UV-Visible absorption spectroscopy, near infrared absorption

spectroscopy, fluorescence spectroscopy, weighing after solvent removal, or just by visual inspection of the darkness of the dispersions. In UV-Vis absorption spectroscopy, the absorption value at 500 nm is often chosen to quantify different CNTs dispersions [21,22]. UV-Visible absorbance spectra of the dispersions were recorded in quartz cylinder (light path length of 5 mm) on a GBC spectrometer (Cintra 10) in the range of 300 to 1000 nm with a scan rate of 500 nm min⁻¹ and a resolution of 0.427 nm. Raman spectra of the samples were recorded at room temperature and atmospheric pressure on Renishaw Raman imaging microscope. The mean crystallite size (D) of the particles was calculated from the XRD line broadening measurement from the Scherrer equation [7]:

$$D = 0.89\lambda / \beta \cos\Theta \quad (1)$$

where λ is the wavelength (CuK α), β is the full width at the half maximum of the HA (211) line and Θ is the diffraction angle.

3. RESULTS AND DISCUSSION

The first step in applying sol-gel methods is the dispersion of CNTs in aqueous ethanol solution, which can be monitored by UV-Vis spectroscopy. CNTs dispersions without ethanol were also prepared accordingly. However, the obtained dispersions were stable only for a few minutes, inspecting the degree of dispersion was made and deposition of the dispersion was conducted. Figure 1 (a,b) shows the UV-Visible absorption spectra of the typical dispersants (SDS [21] as reference and ethanol) and the evolution of the maximum absorbance as a function of the total energy supplied to the solution, which describes the dispersion dynamics of CNTs in aqueous solutions.

The results obtained here were compared with sol-gel method with those obtained by UV-Vis absorption spectroscopy, which is the method most commonly used to analyse carbon nanotube dispersions [14-17]. The curves obtained was very similar to those of the reference. With an increase at the beginning of the sonication process, the value of maximum

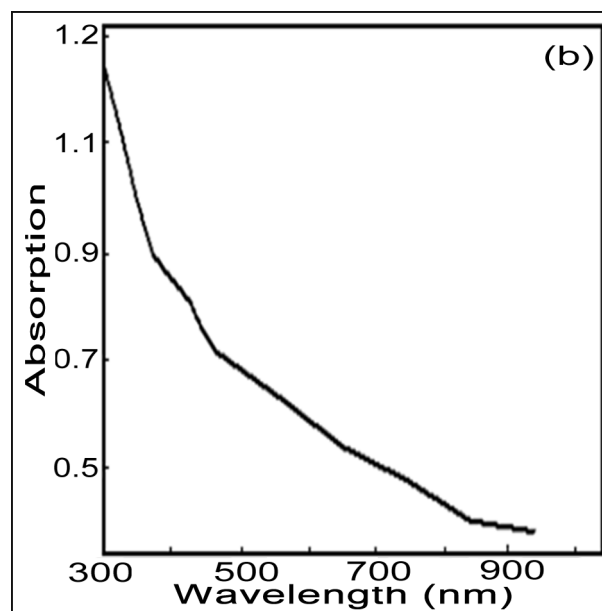
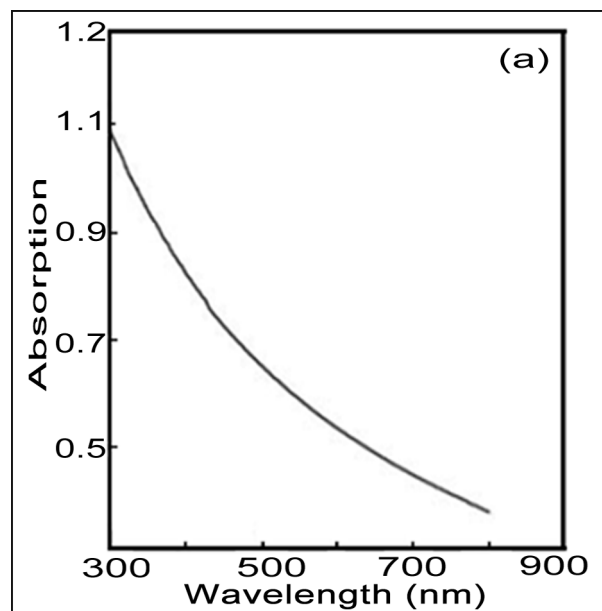


Figure 1: UV-visible absorption spectra of CNTs dispersion using: (a) SDS [21] and (b) Ethanol

absorbance reaches a plateau after a certain amount of energy is supplied, which corresponds to the maximum achievable degree of dispersion of the CNTs in the solution.

The absorptions at 300 nm were 0.98 for SDS [21] and 1.17 for the dispersant used in this paper. Among dispersants, SDS [8, 12] was mainly used to

decrease CNTs aggregative tendency [8].

No crystalline HA phase could be observed in the as-dried state of the gel based on the XRD pattern as is shown in Figure 2, indicating that HA remains amorphous. All the peaks which can be observed in Figure 2 correspond to calcium nitrate implying the incomplete reaction between $\text{Ca}(\text{NO}_3)_2 \cdot 4\text{H}_2\text{O}$ and P_2O_5 . Carbon peaks were not significant for their very low weight fraction in the composite. Crystalline HA powder appears to form only after the heat-treatment at 600°C .

For the crystalline structure of the MWCNTs-HA samples performed by XRD is shown in Figure 3, which shows patterns of HA with 1, 3 and 5 MWCNTs vol%. As shown, most of the diffraction peaks corresponding to HA were observed from Figure 3, at 2θ values 21, 23, 26, 29, 30, 31, 34, 40, 48 and 50° , which were indexed to the (200), (111), (002), (210), (034), (211), (202), (310), (213) and (321) planes, respectively. No peaks corresponding to $\text{Ca}_3(\text{PO}_4)_2$ appear in Figure 3. The peaks positions match well with the diffraction peaks of stoichiometric HA. In addition, as shown in Figure 3, no MWCNTs peaks were found, indicating that small volume fraction of MWCNTs introduced into the solution is difficult to detect within the XRD sensitivity limit. The determined amount of crystallite size for calcined HA by Scherrer equation indicated the average crystal size was ~ 60 nm. As it was reported, the presence of an intense diffraction peak at about 26° which corresponds to (002) plane, indicates the growth of HA crystals along the c-axis [17-19].

It should be noted that the better dispersion of MWCNTs by sol-gel method, and the resulting higher rate of crystallization, account for the larger crystallized fraction. FTIR spectra of MWCNTs, HA, HA with 1, 3 and 5 MWCNTs vol%, are presented in Figure 4. For the purified MWCNTs, a weak peak at 1632 cm^{-1} corresponds to C=C stretch of the nano-tube backbones (Figure 4a). It is considered that the peak at 3560 cm^{-1} corresponds to (OH^-) stretching mode and peaks at 1250 and 1180 cm^{-1} correspond to C-H stretching mode. The weak bands at 1720 cm^{-1} correspond to carbonyl (C=O) group indicating the presence of carboxylic group on the surface of MWCNTs.

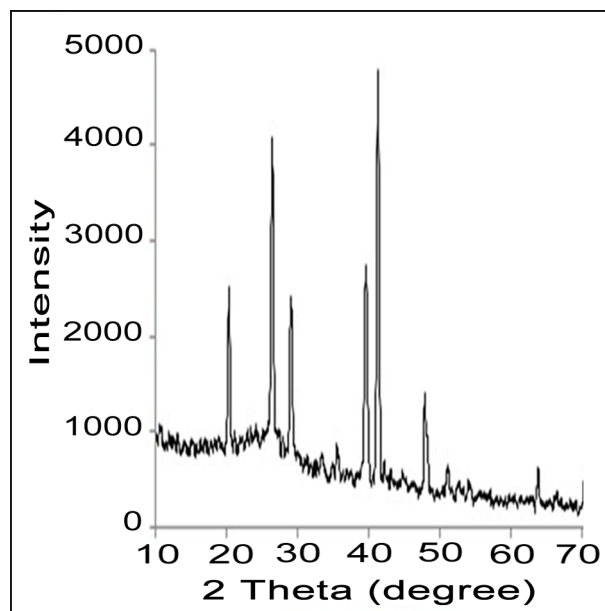


Figure 2: X-ray diffraction (XRD) pattern of the as-dried state of the gel.

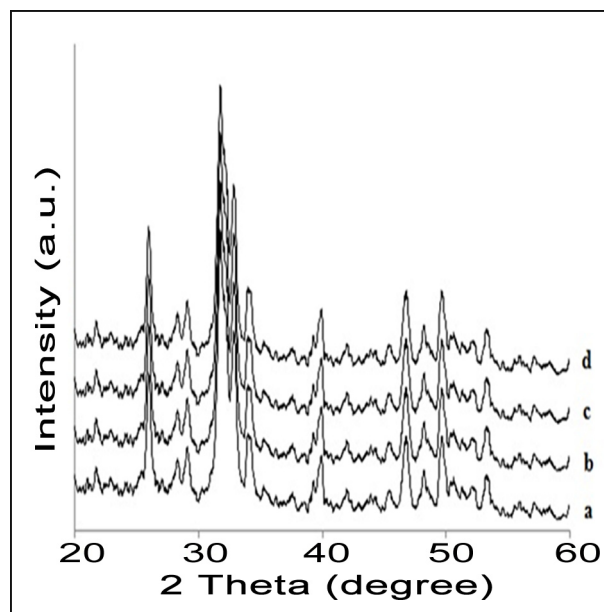


Figure 3: X-ray diffraction (XRD) patterns of (a) HA and different MWCNTs vol% (b) 1, (c) 3 and (d) 5 (Calcination temperature was 600°C for 2h in argon atmosphere)

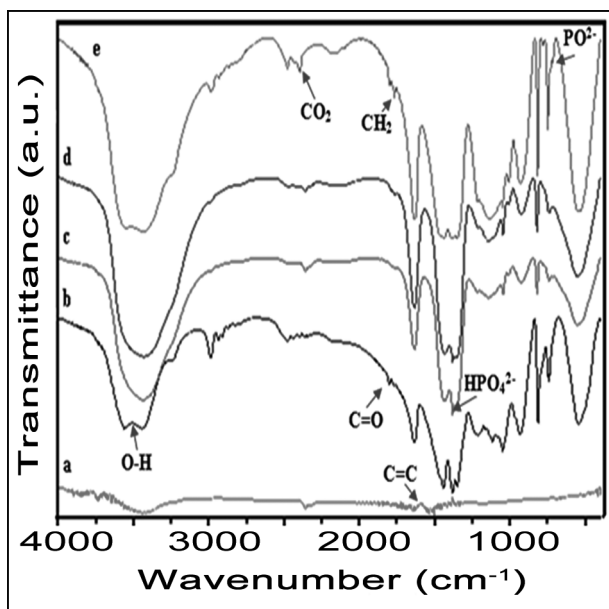


Figure 4: FTIR spectra of (a) MWCNTs, (b) HA (c) HA-1vol% MWCNTs, (d) HA-3vol% MWCNTs and (e) HA-5vol% MWCNTs

The bands in the region of 800-1200 cm^{-1} are probably due to the combination of ν_1 and ν_3 mode of phosphates. The ν_3 PO_4 domain appeared to be the most affected by the possible hydroxyl and even carbonate substitution [16]. Figure 5 (a,b) shows SEM images of smooth surface, open ends of MWCNTs and micrograph of HA-5%MWCNTs dried gel powder. As shown in Figure 5a, big and agglomerated hydroxyapatite are formed primarily by various processes taking place during gel drying. It is also possible that the small particles seen embedded in each agglomerated cluster correspond to calcium nitrate particles, which could be obtained from recrystallization of dissolved calcium nitrate during gel formation. It is known that MWCNTs is easily tend to aggregate because of van der valls force between nanotubes (Figure 5a). It is suggested that the powders synthesized during long aging time were larger than those synthesized during a short aging time, which means that aging could contribute to powder growth and agglomeration.

Figure 6 (a-d) shows SEM micrographs (at different magnification) of powders that were obtained after heat-treatment at 600°C. Arrows highlighting MWCNTs indicate that they disperse

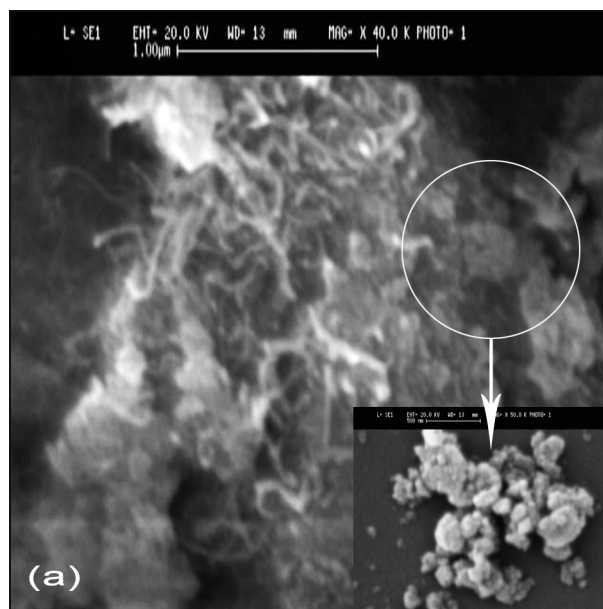
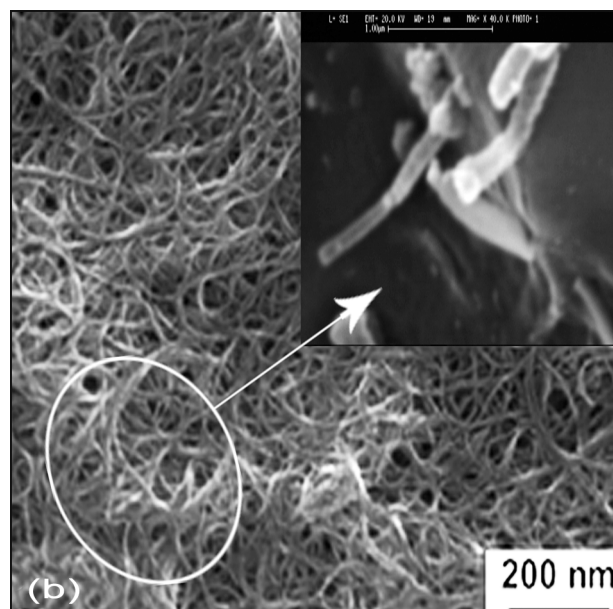


Figure 5: Scanning electron microscopy (SEM) images of (a) HA-5%vol MWCNTs dried gel (at 120°C for 8h) and (b) raw MWCNTs

homogeneously in the HA powder with no diffusion zone around the tubes. The highly magnified images of the composite powder show uniform CNTs distribution and nicely attached to the HA nanoparticles. In Figure 6, the unique multilayered morphology resembling that of natural rock (denser morphology) is formed by biomineralization. This

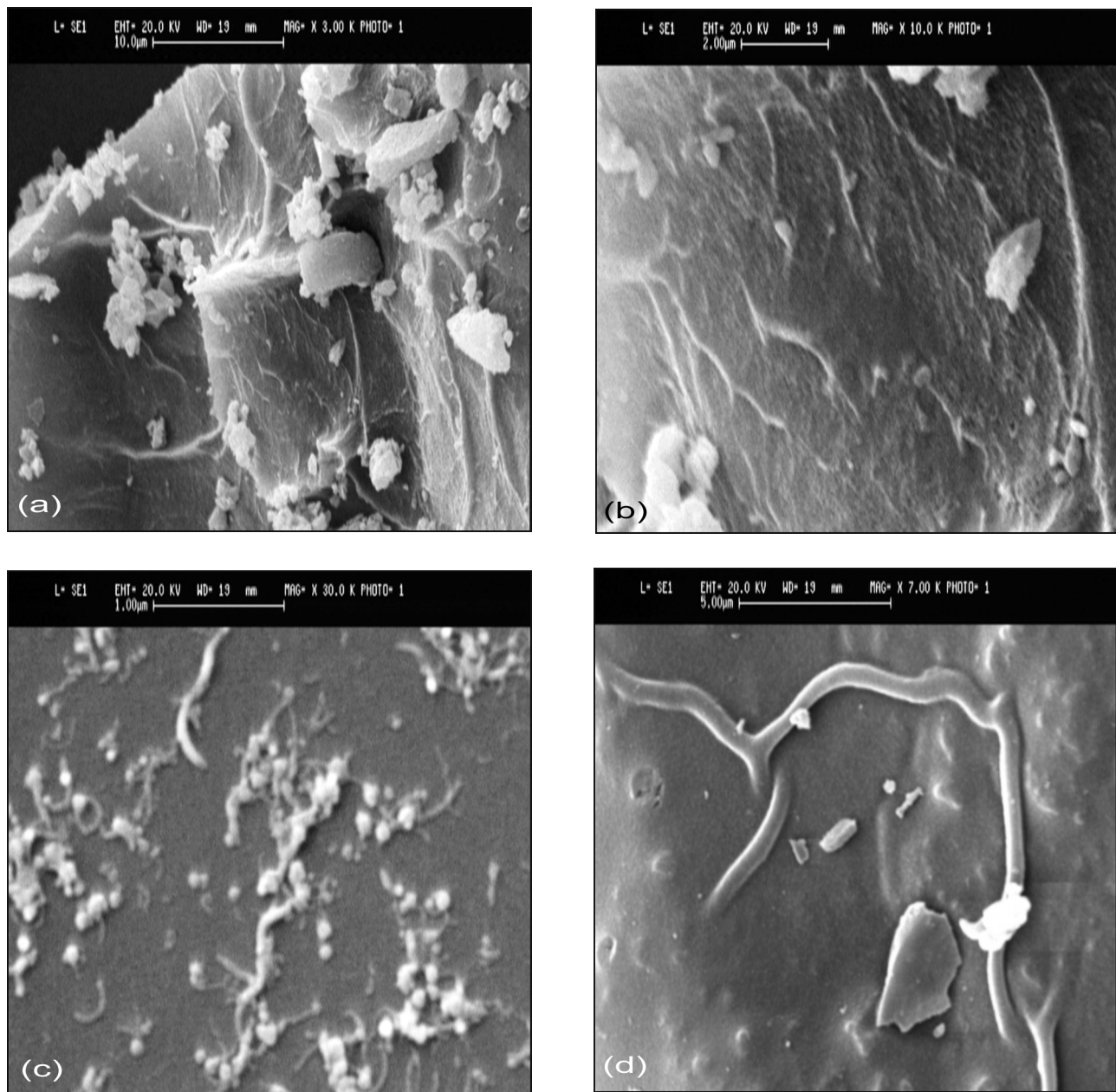


Figure 6: Scanning electron microscope (SEM) images of synthesized HA powder mixed with 5vol%MWCNTs at temperature 600°C for 2h in an inert atmosphere (argon) at different magnifications (a)×5000, (b)×10000, (c)×15000 and (d)×30000

multilayered plate-like morphology may be due to the growth of HA crystals in between the bundle of MWCNTs. It is well known that the MWCNTs are extraordinarily flexible under large strains and resist failure under repeated bending [15]. Therefore, the addition of MWCNTs in the HA matrix allows the fracture energy absorption or dissipation under stress

and significantly improves the fracture toughness of HA composite [14,15].

The presence of MWCNTs affirms pinning and fastening of HA by formation of hooks and bridges (Figure 6d). It is interesting to note that MWCNTs distribute over the worn surface to form a horn-like

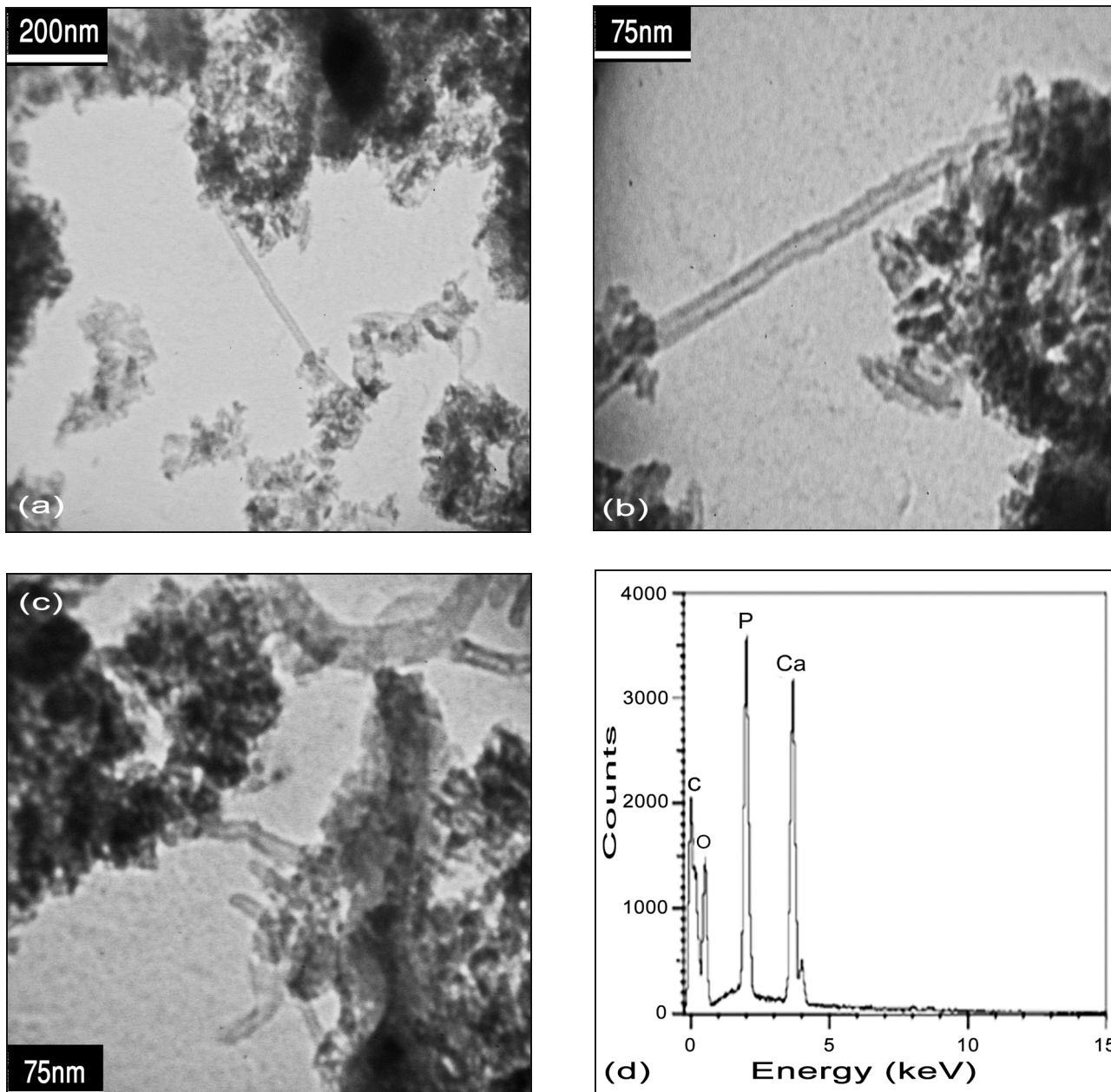


Figure 7: Transmission electron microscopy (TEM) image at magnifications (a) $\times 5000$, (b) $\times 10000$, (c) $\times 15000$ and (d) EDX profiles showing MWCNTs (The anchoring by MWCNTs and showing CNT bridging of splats)

structure under the effect of repeated grinding of the counterpart. Embedded MWCNTs appeared to have strong cohesion with the matrix elements, whereas surface dangling MWCNTs act as energy-absorbing sources. Yet, the field emission SEM micrograph shown in Figure 6 confirmed the existence of CNTs with their originally tubular structure in the composite.

TEM micrographs (Figure 7 (a-c)) of the nanocomposite prepared confirmed that the HA particles showed morphologically rod like and spherical structure. The results of the TEM investigation indicate that also the morphology of the powders is strongly related to Ca/P molar ratio of the sols [19].

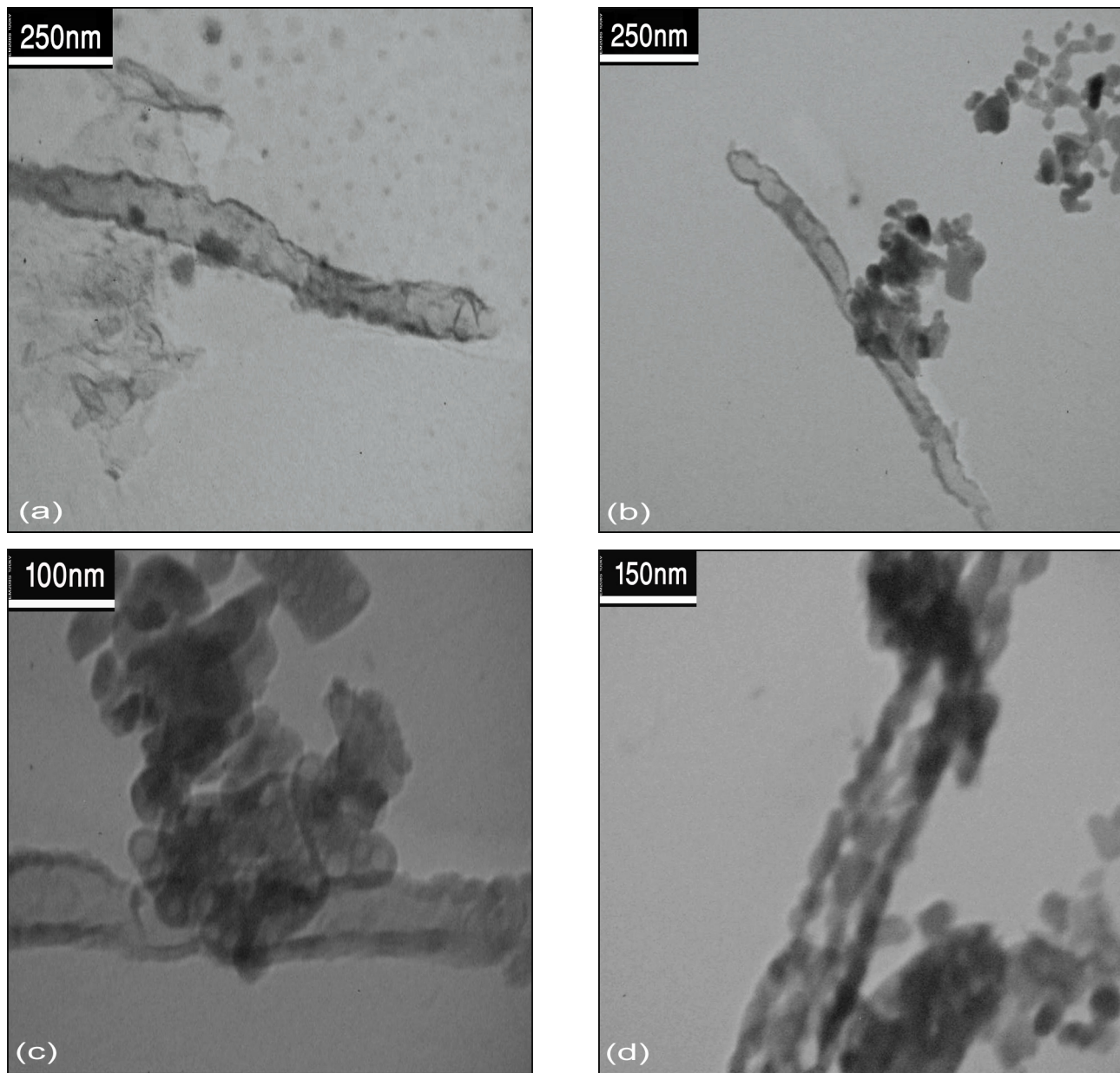


Figure 8: TEM micrograph images of MWCNTs-HA crystal taken at different magnifications (a) $\times 30000$, (b) $\times 25000$, (c) $\times 65000$ and (d) $\times 51000$

Figure 7 also shows that the MWCNTs are slightly bent. These MWCNTs anchor into HA matrix and lead to a significantly higher stress for pulling out and debonding MWCNTs. High magnification analysis was carried out and revealed that the presence of CNTs within the hydroxyapatite matrix, which can improve further the composites fracture toughness, is also attributed to MWCNTs reinforcements which

act as bridges to connect plates [17]. The EDS spectra (Figure 7d), show the constituent elements of the nanocomposite prepared for this study. The presence of the CNTs was confirmed by the peaks for the carbon in the EDS spectrum of the HA-CNTs composite.

This shows that MWCNTs have been successfully introduced into HA matrix. If the dispersion of

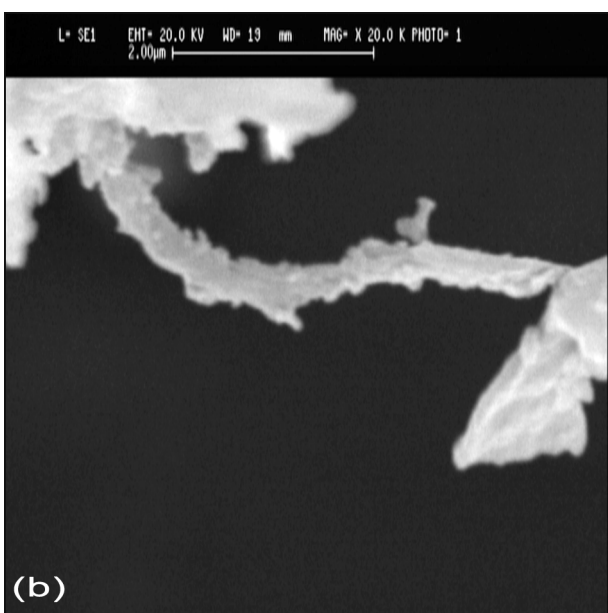
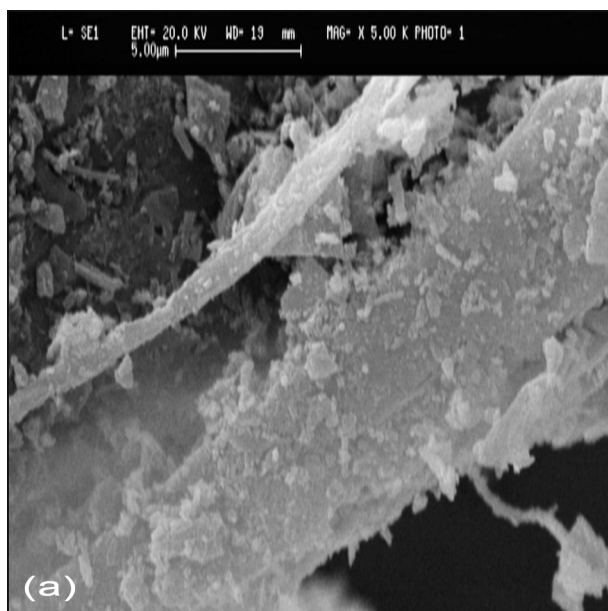


Figure 9: HA precipitation on CNTs present in HA-CNTs at different magnifications (a) $\times 15000$ and (b) $\times 30000$

MWCNTs were further harmonized in the matrix, then the crystallization would begin in a wider scale [5]. It is clearly indicated that MWCNTs still keep their cylindrical graphitic structure due to both high thermal stability and high chemical stability of the MWCNTs. The MWCNTs maintained their typical tubular structure in the HA matrix, as shown in Figure

8. The figure indicates clearly that HA nanoparticles are attached to the surface of MWCNTs. TEM observation supports FTIR spectra (Figure 4) and it can be seen that the length of MWCNTs is of the order of several microns and the hydroxyapatite particles are almost like spherical and irregular hexagon, with the particle size in the range of 50-60 nm. Figure 8c also shows the higher magnification image of HA nanopowders which confirms the presence of MWCNTs with good hollowness, high purity. The amount of attachment appears to be small whereas agglomerated-structure appears over a large area. It should be believed that due to sonication, during sample preparation for TEM, the HA crystals got agglomerated over MWCNTs. Interaction with HA powder resulted in further granulated surface indicating particle attachment on the MWCNTs surface. It is assumed that Ca^{+2} ions can bind with the carboxylic groups on the surface of CNTs. The attachment is confirmed from FTIR measurement (Figure 4). In Figure 9, uniform and nanosized precipitations, from homogeneous solutions containing both Ca and P on CNTs surface are observable (most of the CNTs are actually covered by very fine HA powders). As a matter of fact, HA precipitation on CNTs surface renders them bioactive. Precipitation of HA (Figure 9b) on the outer wall of CNTs when exposed to simulated body fluids has been documented by other researchers as well [14,23-25].

The SEM micrograph of HA powders suggests that the composite sample is composed of agglomerates of broad size distribution (Figure 10a). The mean aggregation size of the synthesis grains was approximately 500 nm-5 μm . As shown in Figure 10b at higher magnification the smaller the particles size the more uniform distribution for the HA crystallites in the system is achieved.

The agglomeration of these nanoparticles is attributed to van der Waals force of attraction [15]. TEM micrographs observation confirmed that HA showed similar morphological rod like structure (nano-sized ellipse-like morphology). The apparent agglomerates of about 100 nm in size were observed (Figure 10c). Close inspection revealed nano-structure of nano-crystals of about 50-60 nm in size (Figure 10d).

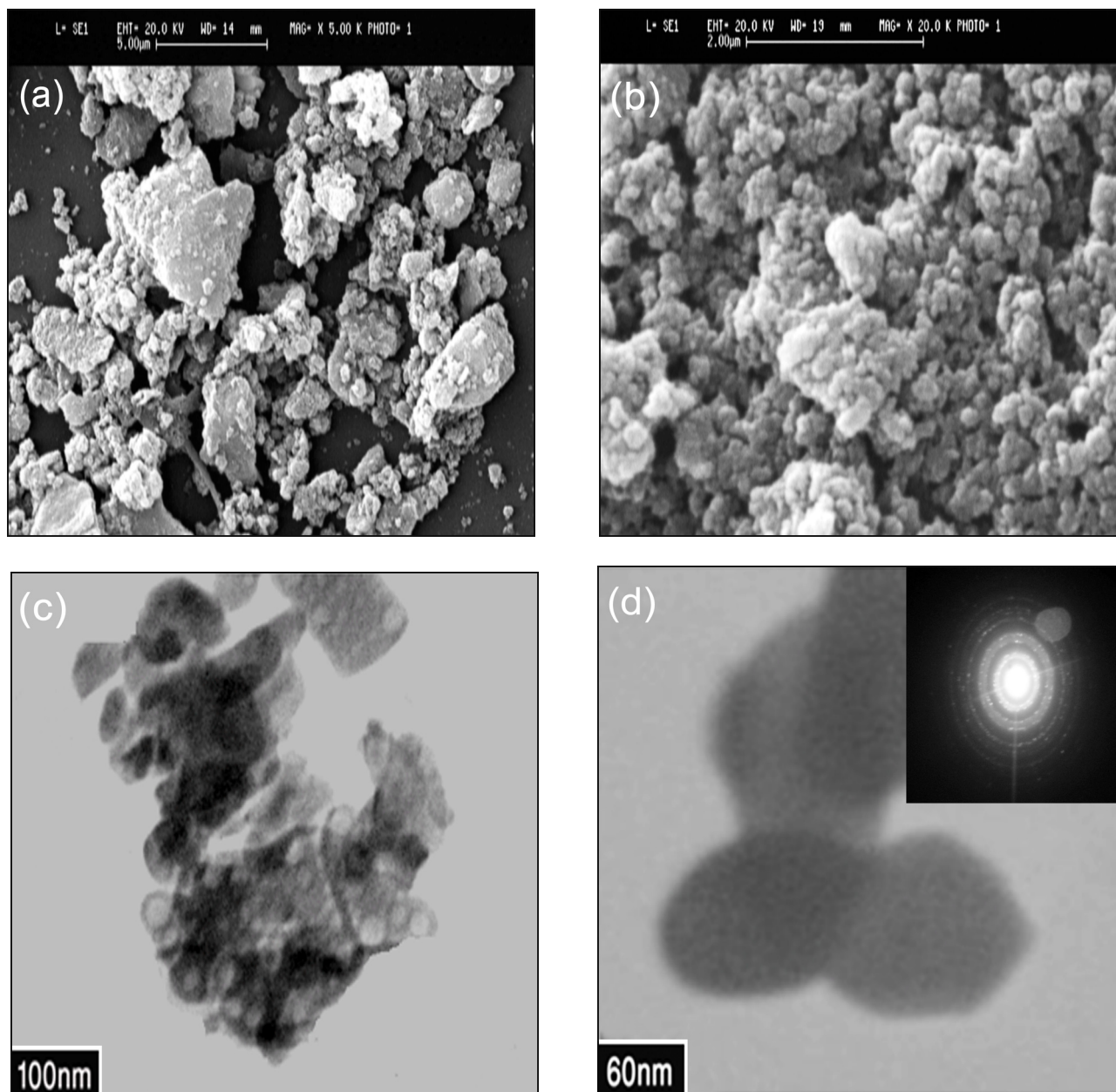


Figure 10: Electron microscopy images of hydroxyapatite nano-powders after heat treatment: (a) SEM, (b) FESEM, (c) TEM photomicrograph and (d) show corresponding electron diffraction patterns.

Selected area electron diffraction (SAED) patterns of the HA crystals showed that the (211) planes were aligned with the crystals axis, indicating that the crystal growth was along the c-axis direction, which was consistent with the XRD data discussed above. The as-obtained composite powder was also characterized by Raman spectroscopy in

detail to validate the presence of CNTs. The Raman spectroscopy (Figure 11 (a,b)) performed on the composite powders distinctly exhibited two peaks (1349.5 and 1572.7 cm^{-1}) for multi-walled CNTs, which were associated with the vibrations of carbon atoms with dangling bonds for the in plane terminations of the disordered

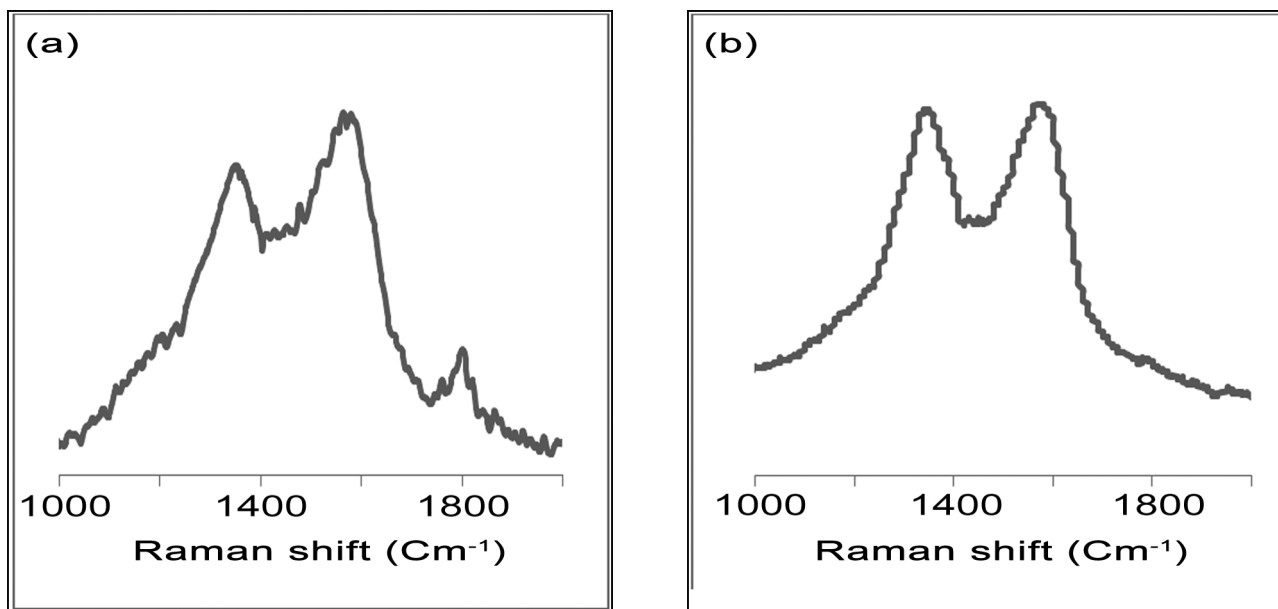


Figure 11: Raman spectrum of the as-obtained composite powders of samples (a) HA+5%CNTs and (b) CNTs.

graphite and the vibrations in all sp^2 bonded carbon atoms in a 2-dimensional hexagonal lattice, respectively. The intensity ratio of D to G band (I_D/I_G) was calculated to be 0.71 Figure 11a. The relatively low intensity of D to G-band implies that the obtained CNTs were mainly composed of well-crystallized graphite, in agreement with the SEM and TEM observations. The intensity of each peak was found to increase with an increase of CNTs in hydroxyapatite matrix.

4. CONCLUSION

In this study, carbon nanotubes were dispersed in the hydroxyapatite (HA) matrix using ethanol as dispersant (stable aqueous colloidal dispersions of CNTs were obtained with the aid of ethanol) and the application of sol-gel process and its effects on the microstructure were investigated. It has also been shown that the aqueous sol-gel processing is a suitable synthetic procedure for producing homogeneous single phase HA with the desired morphological properties. Results showed that the synthesis of HA particles in the MWCNTs sol, which was prepared in advance, lead to an excellent dispersion of MWCNTs

in HA matrix. Average HA crystal sizes measured by XRD and TEM observation showed the proximate value of 50 to 60 nm.

REFERENCES

1. M. Meyyappan, NASA AR Center, Moffett Field, CA, CRC Press LLC, 2005, pp. 2-21.
2. Y. Gogotsi, Drexel University, Philadelphia, Pennsylvania, USA, Taylor and Francis Group, LLC, 2006, pp. 41-70.
3. E. T. Thostenson, Z. Ren, T. W. Chou, *Comp. Sci. Technol.* 61 (2001) 1899-1912.
4. S. Pegel, P. Potschke, G. Petzold, I. Alig, S. M. Dudkin, D. Lellinger, *Polymer* 49 (2008) 974-984.
5. T. Wei, Z. Fan, G. Luo, F. Wei, *Mater. Lett.* 62 (2008) 641-644.
6. G. Yamamoto, M. Omori, K. Yokomizo, T. Hashida, K. Adachi, *Mater. Sci. Eng. B* 148 (2008) 265-269.
7. Y. Chen, Y. Q. Zhang, T. H. Zhang, C. H. Gan, C. Y. Zheng, G. Yu, *Carbon* 44 (2006) 37-45.